

Photon echo induced by two-exciton coherence in a GaAs quantum well

T. Saiki* and M. Kuwata-Gonokami†

Department of Applied Physics, University of Tokyo, 7-3-1 Hongo, Bunkyo-ku, Tokyo 113, Japan

T. Matsusue‡

Institute of Industrial Science, University of Tokyo, 7-22-1 Roppongi, Minato-ku, Tokyo 106, Japan

H. Sakaki

*Institute of Industrial Science, University of Tokyo, 7-22-1 Roppongi, Minato-ku, Tokyo 106, Japan;
Research Center for Advanced Science and Technology, University of Tokyo, 4-6-1 Komaba, Meguro-ku, Tokyo 153, Japan;
and Quantum Wave Project, ERATO, Research Development Corporation of Japan, 4-3-24 Komaba, Tokyo 153, Japan*

(Received 15 July 1993; revised manuscript received 8 December 1993)

Excitonic nonlinearities in the weak-excitation limit condition are examined with time-integrated and time-resolved four-wave mixing (FWM). Below an excitation of 3×10^9 excitons/cm², coherent third-order processes prevail. Echo-type signals are observed in parallel and perpendicular polarization configurations. The coherent process induced by the two-photon coherence of the two-exciton state is attributable to signals in the perpendicular configuration. The polarization dependences of a temporal profile and the intensity of FWM signals are well explained with third-order perturbational analysis that takes into account the two-exciton states and inhomogeneity.

The importance of excitonic nonlinearities has been stressed because of their large magnitude as well as their fast response.¹ In the high-density excitation regime, a many-body interaction is treated by a mean-field approximation of a set of semiconductor Bloch equations (SBE's).² Such a mean-field approximation is valid when the interaction energy between two excitons, Ω_{int} , is much smaller than the exciton homogeneous width Γ . In GaAs, the binding of two excitons is very weak and Ω_{int} is reported to be of the order of 1 meV.^{3,4} In conventional experiments such as pump and probe measurements, the pumping power must be strong in order to get a sufficient signal. The strong pump beam induces the exciton dephasing and we get the above condition. Thus the SBE's can explain well the essential features of coherent and incoherent processes caused by the many-body interaction between carriers and excitons.⁵⁻⁸ In the weak-excitation regime, however, the homogeneous width of the exciton is known to be of the order of 0.05 meV,⁹ which is smaller than the interaction energy of two excitons. Although several attempts have been reported, the excitonic nonlinear responses in the weak-excitation limit have not been fully explored, neither experimentally nor theoretically.

Two-pulse four-wave mixing (FWM) is a method suitable for the study of the nonlinear responses in the femtosecond region. The perpendicular configuration of the two-pulse FWM method, where the polarizations of two beams are linear and perpendicular to each other, was often used to avoid the incoherent effect such as thermal grating.¹⁰ Recently, it has been identified that the signals in the parallel and perpendicular configurations have different features.^{9,11-13} In time-integrated (TI) FWM experiments, differences in the decay times as well as in the signal intensities have been observed for various sys-

tems. In a time-resolved (TR) FWM experiment, echo-type signals are observed in parallel configuration, while the free-induction-decay-type signals are observed in perpendicular configuration.⁹ In spite of many attempts to explain these features, there has not yet been a systematic investigation to explain all the features consistently.

In this paper, we present experimental results of the polarization dependences of TI and TR FWM of strict third-order regime in GaAs quantum well (QW). We present evidence of a photon-echo process that arises from the two-photon coherence of two excitons with phase correlation in the inhomogeneously broadened system.

If the FWM signal follows the third-order power dependences over a wide range of power of input pulses, we can describe the FWM processes with the third-order perturbational method which enables us to follow the change of the material states step by step.¹⁴ The relevant states of the crystal are ground state, one-exciton state, and two-exciton state. The two-exciton state involves a stable biexciton state,^{3,4,15,16} its excited states, and repulsively interacting unbound two-exciton states. Two optical pulses with wave vector $\mathbf{k}_1, \mathbf{k}_2$ and with polarization $\mathbf{E}_1, \mathbf{E}_2$ generate third-order nonlinear polarization in the sample. The third-order nonlinear polarization emits signal photons in the direction of $2\mathbf{k}_1 - \mathbf{k}_2$. Now we assume that the excitons are isotropic inside the plane of wells. Thus the optically active two-exciton states (x - and y -polarized exciton states) are equivalent. There are two different processes which generate coherently a FWM signal in the direction of $2\mathbf{k}_1 - \mathbf{k}_2$. One is the two-level-like process [Fig. 1(a)], where only a one-exciton state is involved. The other is the process associated with the two-photon coherence of the two-exciton state where two excitons have phase correlation through the Coulomb

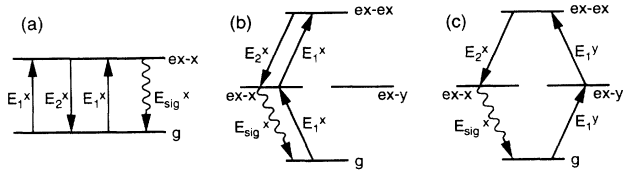


FIG. 1. Optical processes of the four-wave mixing for parallel [(a) and (b)] and perpendicular (c) polarization configurations. The levels g , $ex-x$ ($-y$), and $ex-ex$ represent the ground state, x - (y -) polarized one-exciton state and two-exciton state, respectively. E_i^j represents the electric field of the i th pulse with j polarization.

and exchange interaction [Figs. 1(b) and 1(c)]. The two-exciton state can support the two-photon coherence within the phase correlation memory time, which is the dephasing time of the two-exciton state. In the perpendicular polarization configuration, where E_1 is y -polarized and E_2 is x -polarized, the former process (two-level-like process) does not occur. Only the latter process can contribute to the signal. Such a process can be expressed with the four-level diagram shown in Fig. 1(c), which was first introduced to show the two-photon polarization rotation effect of the Γ_1 biexciton in CuCl.¹⁷ In the two-exciton state, the exciton wave functions are modified and the total wave function of the two-exciton state has its characteristic symmetry. For example, the lowest bound biexciton state in a cubic crystal has the total symmetry (Γ_1 symmetry). Therefore, the two-exciton state created by the absorption of two x -polarized photons can be deexcited by emitting two y -polarized photons [Fig. 1(c)]. Hence, the signal in perpendicular configuration is a good measure for detecting the two-photon coherence of the two-exciton state.

The GaAs QW sample is grown by molecular-beam epitaxy with the growth interruption.¹⁸ It consists of 30 periods of 100-Å GaAs wells and 80-Å AlAs barriers. The GaAs substrate was etched to allow the transmission of light. The transmission spectrum of the heavy-hole exciton line is shown in Fig. 2(a). This line, whose width is

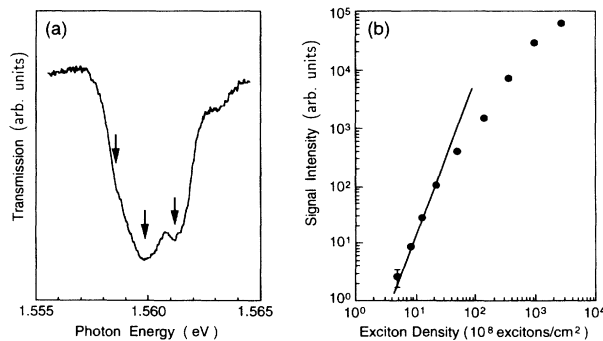


FIG. 2. (a) Transmission spectrum of heavy-hole excitons of GaAs quantum well of 100-Å well width. Downward arrows indicate the exciton structures caused by one-monolayer fluctuation of the well width. (b) Excitation-power dependence of the signal intensity for parallel configuration. Straight line indicates cubic behavior.

3.5 meV, has three structures which correspond to the different confinement energies caused by the one-monolayer fluctuation of the well width. This shows that the heavy-hole exciton in our sample is inhomogeneously broadened. The homogeneous linewidth is evaluated as 0.04 meV as we will show below. We use a cw passively mode-locked Ti:sapphire laser (Coherent Mira 900) with a pulse duration of 170 fs and linewidth of 7.5 meV. We measure the TI and TR FWM signal as a function of delay time T , which is the interval between the two incident pulses. The sign of T is positive when pulse 2 precedes pulse 1. All the measurements are performed at 10 K. The FWM signals show the third-order power dependence up to excitation of 500 kW/cm² which corresponds to the exciton density of 3×10^9 excitons/cm² as shown in Fig. 2(b). Below this power level, all the temporal responses are unchanged.

Figure 3 shows the TI FWM signal as a function of T . The center frequency of the pulse is 1.559 eV. We fit slow components of the data with the function, $I_j(T) = I_j \exp(-T/\tau_j)$, where $j = \parallel, \perp$ for parallel and perpendicular configurations, respectively. The decay time in the perpendicular configuration, τ_{\perp} , is 0.8 ps which is much shorter than τ_{\parallel} (3.9 ps). The polarization-dependent decay rates are consistent with the results reported previously.^{9,11-13} The observed ratio I_{\parallel}/I_{\perp} is about 10 which is much smaller than the value in ZnSe but almost the same as the value of bulk GaAs reported recently.¹⁹ Figures 4(b) and 4(c), respectively, show the TR FWM signals for parallel and perpendicular configuration at various delay time T . In contrast to the previous report,⁹ photon-echo-type responses are observed in both polarization configurations. With the increase of the pulse interval T , total signal intensity, which is the area of the TR FWM signal, in perpendicular configuration decays more rapidly than in the case of the parallel configuration. This is consistent with the results of the TI FWM experiment. From the echo-pulse width, the full width of the inhomogeneous distribution can be estimated. In our case, an echo-pulse width of 0.7 ps gives an inhomogeneous width of 3.5 meV. This value agrees with the spectral width of the transmission spectrum.

Figure 4(a) shows the time ordering of the light-matter interaction in the coherent third-order processes of the FWM with the double-sided Feynman diagram representation. For the perpendicular configuration, the only relevant process that generates the FWM signal in the

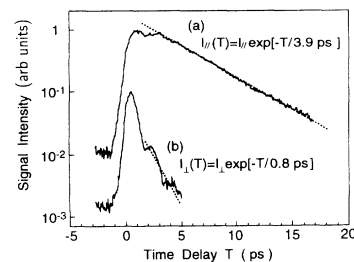


FIG. 3. TI FWM signal as a function of delay between first and second pulses for parallel (a) and perpendicular (b) configurations.

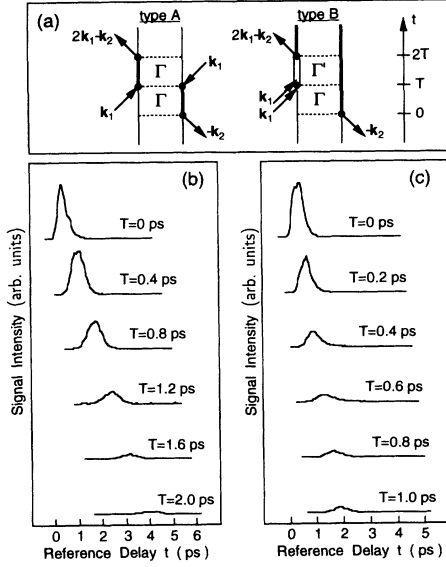


FIG. 4. (a) Double-sided Feynman diagram corresponding to photon echo for ordinary two-level-like process (type A) and for three-level-like process due to two-exciton coherence (type B). Bold and double lines represent the one-exciton state and two-exciton state, respectively. TR FWM signals at various time delay T , for parallel (b) and perpendicular (c) configurations.

positive delay, $T > 0$, is illustrated as type B. The third-order nonlinear polarization caused by the coherence between the one-exciton state and the two-exciton state emits the FWM signal. We denote the dephasing rate of this third-order coherence as Γ' . In parallel configuration, the two-level-like process (type A) can also contribute to the signal. The signals are emitted via the third-order polarization between the ground state and one-exciton state. With this picture, we can formulate temporal profiles of third-order signals of TR FWM as well as TI FWM for both the homogeneous and inhomogeneous cases.²⁰

In the inhomogeneously broadened system, TR FWM signals are photon-echo-type in both polarization configurations. In the ordinary two-level-like photon-echo process (type A), pulse 1 is incident at $t=0$ and pulse 2 at $t=T$, the third-order polarization is reconstructed at $t=2T$. The decay rate of the TI FWM signal depends on the dephasing of the two-exciton state during the time between $t=T$ and $t=2T$ as well as the exciton coherence from $t=0$ to $t=T$. Now we take the state with the interaction energy Ω_{int} and dephasing rate of Γ' as a representative state for simplicity; TI FWM signals can be expressed as follows:

$$I_{\parallel}(T) = C \{ (2\alpha + f)^2 \exp(-4\Gamma T) + f^2 \exp[-2(\Gamma + \Gamma')T] - 2(2\alpha + f)f \cos(\Omega_{\text{int}}T) \exp[-(3\Gamma + \Gamma')T] \}, \quad (1)$$

$$I_{\perp}(T) = C f^2 \exp[-2(\Gamma + \Gamma')T], \quad (2)$$

where the parameter α is the phase space filling factor²¹ and f is the enhancement factor of oscillator strength between the one-exciton state and the two-exciton state, measured with the oscillator strength of the single exciton transition.²² The factor C contains the factors $|E_1|^4 |E_2|^2$ and $[1 + \Phi(\delta T/\sqrt{2})]$, where $\Phi(x)$ is the error function and δ is the inhomogeneous width. The calculation yields the slowest term as $I_{\perp}(T) = I_{\perp} \exp[-2(\Gamma + \Gamma')T]$ and, for parallel configuration, $I_{\parallel}(T) = I_{\parallel} \exp[-4\Gamma T]$. In GaAs, the binding of two excitons is very weak and they easily dissociate into unbound states. Therefore, Γ' is much larger than the exciton dephasing rate Γ . This is the reason why we observed very fast decay in the perpendicular configuration of TI FWM. Using the model potential of Ref. 23 we estimated the factor f of the bound state and obtained the value of 3.4. With this value we obtain the ratio $I_{\parallel}/I_{\perp} \sim 9.2$ by Eqs. (1) and (2). This is close to the observed value.

In the case of a homogeneously broadened system, the profile of the time-resolved signal becomes free-induction-decay-type in both polarization configurations. The emission starts at $t=T$ with a decay constant Γ in the parallel configuration and Γ' in the perpendicular configuration. Therefore the time-integrated signals show the dependence on T as $I(T) \sim \exp[-2\Gamma T]$ irrespective of the polarization configuration. In ZnSe, we observed polarization-independent decay of TI FWM and free-induction-decay-type signal of TR FWM.²⁴ This is the reason why the polarization dependence of the decay rates in TI FWM strongly depends on the sample quality. In fact, the same decay time in TI FWM in both configurations is reported in GaAs QW's of extremely homogeneous samples.¹²

Sample-dependent inhomogeneity causes the qualitative difference in the TR FWM experiment. Now we consider the system of slight inhomogeneous broadening, where the inhomogeneous width is larger than Γ but comparable with Γ' . In such a case, the two-level-like process of type A leads to the photon-echo-type TR FWM signal. On the other hand, the reconstruction of the echo signal is incomplete in the three-level-like process of type B. Thus the TR FWM in perpendicular configuration becomes free-induction-decay-type rather than echo-type. This may cause the qualitative difference of the TR FWM signal in parallel and perpendicular configurations.⁹ These explanations with perturbational analyses are consistent with the present experimental results as well as the previous results.^{9,11-13}

Recently, Wang *et al.* examined the intensity dependence of the ratio of I_{\parallel}/I_{\perp} in bulk GaAs and showed that incoherent process such as density-dependent exciton dephasing caused by the exciton-exciton scattering may largely contribute to the FWM of parallel configuration.¹⁹ In this process, the second pulse is scattered to the $2k_1 - k_2$ direction by the index grating caused by the periodic modulation of the imaginary part of the self-energy correction. This process should lead to prompt signals in the TR FWM experiment. In our experiment, however, echo-type signals without any prompt signals

are observed. And, moreover, we confirm the intensity-independent dephasing rate below the excitation density of 3×10^9 excitons/cm². This implies that such types of incoherent processes are irrelevant to our experiment and only the coherent processes occur in the truly third-order region.

The authors are grateful to Dr. K. Ema and to Professor E. Hanamura for enlightening discussions. This work was supported by the Grant-in-Aid for General Scientific Research and Grant-in-Aid for Developmental Scientific Research from the Ministry of Education, Science and Culture, Japan.

*Present address: Kanagawa Academy of Science and Technology, 3-2-1 Sakado, Takatsu-ku, Kawasaki, Kanagawa 213, Japan.

†Author to whom correspondence should be addressed.

‡Present address: Department of Material Science, Faculty of Engineering, Chiba University, 1-33 Yayoi-cho, Inage-ku, Chiba 263, Japan.

¹E. Hanamura, Phys. Rev. B **38**, 1228 (1988).

²M. Lindberg and S. W. Koch, Phys. Rev. B **38**, 3342 (1988).

³R. T. Phillips, D. J. Lovering, G. J. Denton, and G. W. Smith, Phys. Rev. B **45**, 4308 (1992); D. J. Lovering, R. T. Phillips, G. J. Denton, and G. W. Smith, Phys. Rev. Lett. **68**, 1880 (1992).

⁴K.-H. Pantke, D. Oberhauser, V. G. Lyssenko, J. M. Hvam, and G. Weimann, Phys. Rev. B **47**, 2413 (1993).

⁵S. Schmitt-Rink and D. S. Chemla, Phys. Rev. Lett. **57**, 2752 (1986); S. Schmitt-Rink, D. S. Chemla, and H. Haug, Phys. Rev. B **37**, 941 (1988).

⁶M. Wegener, D. S. Chemla, S. Schmitt-Rink, and W. Schäfer, Phys. Rev. A **42**, 5675 (1990).

⁷S. Weiss, M.-A. Mycek, J.-Y. Bigot, S. Schmitt-Rink, and D. S. Chemla, Phys. Rev. Lett. **69**, 2685 (1992).

⁸Dai-Sik Kim, Jagdeep Shah, T. C. Damen, W. Schäfer, F. Jahnke, S. Schmitt-Rink, and K. Köhler, Phys. Rev. Lett. **69**, 2725 (1992).

⁹S. T. Cundiff, H. Wang, and D. G. Steel, Phys. Rev. B **46**, 7245 (1992); S. T. Cundiff and D. G. Steel, IEEE J. Quantum Electron. **28**, 2423 (1992).

¹⁰K. Leo, E. O. Göbel, T. C. Damen, J. Shah, S. Schmitt-Rink, W. Schäfer, J. F. Müller, K. Köhler, and P. Ganser, Phys.

Rev. B **44**, 5726 (1991).

¹¹S. Schmitt-Rink, D. Bennhard, V. Heuckeroth, P. Thomas, P. Haring, G. Maidorn, H. Bakker, K. Leo, Dai-Sik Kim, Jagdeep Shah, and K. Köhler, Phys. Rev. B **46**, 10460 (1992).

¹²D. Bennhardt, P. Thomas, R. Eccleston, E. J. Mayer, and J. Kuhl, Phys. Rev. B **47**, 13485 (1993).

¹³Henry H. Yaffe, Yehiam Prior, J. P. Harbison, and L. T. Florez, J. Opt. Soc. Am. B **10**, 578 (1993).

¹⁴M. Kuwata-Gonokami and T. Saiki, in *Nonlinear Optics Fundamentals, Materials and Devices*, edited by S. Miyata (North-Holland, Amsterdam, 1992), p. 329.

¹⁵B. F. Feuerbacher, J. Kuhl, and K. Ploog, Phys. Rev. B **43**, 2439 (1991).

¹⁶G. Finkelstein, S. Bar-Ad, O. Carmel, I. Bar-Joseph, and Y. Levinson, Phys. Rev. B **47**, 12964 (1993).

¹⁷M. Kuwata and N. Nagasawa, J. Phys. Soc. Jpn. **51**, 2598 (1982).

¹⁸T. Matsusue, H. Akiyama, and H. Sakaki, Superlatt. Microstruct. **13**, 41 (1993).

¹⁹H. Wang, K. Ferrio, D. G. Steel, Y. Z. Hu, R. Binder, and S. W. Koch, Phys. Rev. Lett. **71**, 1261 (1993).

²⁰T. Saiki, Ph.D. dissertation, University of Tokyo, 1993.

²¹S. Schmitt-Rink, D. S. Chemla, and D. A. B. Miller, Phys. Rev. B **32**, 6601 (1985).

²²J.-Y. Bigot, A. Daunois, J. Oberlé, and J.-C. Merle, Phys. Rev. Lett. **71**, 1820 (1993).

²³I. A. Karp and S. A. Moskalenko, Fiz. Tekh. Poluprovodn. **8**, 285 (1974) [Sov. Phys. Semicond. **8**, 183 (1974)].

²⁴T. Saiki *et al.*, J. Cryst. Growth (to be published).